Coulomb Plasmas in Outer Envelopes of Neutron Stars

A.Y. Potekhin^a, G. Chabrier^b, D.G. Yakovlev^a

^aIoffe Physical-Technical Institute, 194021 St. Petersburg, Russia ^bEcole Normale Supérieure de Lyon, CRAL, 69364 Lyon Cedex 07, France e-mail: palex@astro.ioffe.rssi.ru

Abstract

Outer envelopes of neutron stars consist mostly of fully ionized, strongly coupled Coulomb plasmas characterized by typical densities $\rho \sim 10^4 - 10^{11}~{\rm g\,cm^{-3}}$ and temperatures $T \sim 10^4 - 10^9~{\rm K}$. Many neutron stars possess magnetic fields $B \sim 10^{11} - 10^{14}~{\rm G}$. Recent theoretical advances allow one to calculate thermodynamic functions and electron transport coefficients for such plasmas with an accuracy required for theoretical interpretation of observations.

1 Overview

Envelopes of neutron stars (NSs) are divided in the inner and outer envelopes. Properties of the inner envelopes are outlined in a companion paper [1]. Here we focus on the outer ones, at typical densities $\rho \sim 10^4 - 10^{11} \ \mathrm{g \ cm^{-3}}$ and temperatures $T \sim 10^4 - 10^9 \ \mathrm{K}$. These envelopes are relatively thin, but they affect significantly NS evolution. In particular, they provide thermal insulation of stellar interiors.

Bulk properties of the NS envelopes (pressure P, internal energy U) are determined mainly by degenerate electron gas. The electrons are relativistic at $x_r \gtrsim 1$, where $x_r \equiv \hbar k_{\rm F}/mc \approx (\rho_6 Z/A)^{1/3}$, $k_{\rm F} = (3\pi^2 n_{\rm e})^{1/3}$ is the Fermi wave number, m is the electron mass, $n_{\rm e} = Z n_{\rm i}$ is the electron number density, $\rho_6 \equiv \rho/10^6$ g cm⁻³, Z and A are the ion charge and mass numbers, respectively. Degeneracy is strong at $T \ll T_{\rm F} = (\epsilon_{\rm F} - mc^2)/k_{\rm B}$, where $\epsilon_{\rm F} = mc^2\gamma_{\rm r}$ and $\gamma_{\rm r} = \sqrt{1 + x_{\rm r}^2}$ is the Lorentz factor.

The ionic component of the plasma can form either strongly coupled Coulomb liquid or solid, classical or quantum. The classical ion coupling parameter is $\Gamma = (Ze)^2/ak_{\rm B}T$, where a is the ion-sphere radius $(\frac{4\pi}{3}a^3 = n_{\rm i}^{-1})$. The ions form a crystal if Γ exceeds some critical value Γ_m (see below). The quantization of ionic motion becomes important at $T \ll T_{\rm p}$, where $T_{\rm p} = \hbar \sqrt{4\pi n_{\rm i} Z^2 e^2/M}/k_{\rm B}$ is the ion plasma temperature, and M is the ion mass. The ionic contribution determines specific heat C_V , unless $T \ll T_{\rm p}$.

The ions and electrons are coupled together through the electron response (screening). The inverse screening (Thomas–Fermi) length is $k_{\rm TF} = (4\pi e^2 \, \partial n_{\rm e}/\partial \mu)^{1/2}$, where μ is the electron chemical potential. If $T \ll T_{\rm F}$, then $\mu \approx \epsilon_{\rm F}$ and $k_{\rm TF}^2/k_{\rm F}^2 \approx 4(\alpha/\pi)\,\gamma_{\rm r}/x_{\rm r}$, where α is the fine structure constant. Note that $\gamma_{\rm r}/x_{\rm r} \to 1$ at $x_{\rm r} \gg 1$; therefore the screening effects do not vanish even at high densities.

Thermodynamic properties are altered by the magnetic field B in the case where the Landau quantization of transverse electron motion is important. The field is called strongly quantizing when it sets all electrons on the ground Landau level. This occurs at $\rho < \rho_B$ and $T \ll T_B$ (see, e.g., ref. [2]), where $\rho_B \approx 7045 \, (A/Z) \, B_{12}^{3/2} \, {\rm g \, cm^{-3}}, T_B \approx 1.343 \times 10^8 (B_{12}/\gamma_{\rm r})$ K, and $B_{12} \equiv B/10^{12}$ G. Weakly quantizing fields $(\rho_B < \rho)$ do not significantly alter P and U but cause oscillations of C_V , other second-order quantities, and electron transport coefficients with increasing density.

Characteristic domains in the ρ -T diagram are shown in Figure 1. The short-dashed lines on the left panel indicate the region of partial ionization. The dot-dashed lines correspond to $\Gamma = 1$ (upper lines) and $\Gamma = 175$ (liquid/solid phase transition). Long-dashed lines on the right panel separate three ρ -T regions where the magnetic field is strongly quantizing (to the left of ρ_B and considerably below T_B), weakly quantizing (to the right of ρ_B at $T \lesssim T_B$), or classical (much above T_B).

The dotted lines in Fig. 1 show profiles $T(\rho)$ in the envelope of a "canonical" NS with mass $1.4 M_{\odot}$ and radius 10 km, and with an effective surface temperature $T_{\rm s} = 5 \times 10^5 \, \mathrm{K}$ or 2×10^6 K (the values of $T_{\rm s6} \equiv T_{\rm s}/10^6$ K are marked near these curves). Typical temperatures of isolated NSs are believed to lie in the hatched region between these two lines. In a magnetized NS, $T(\rho)$ depends on strength as well as direction of the magnetic field. Therefore on the right panel we show

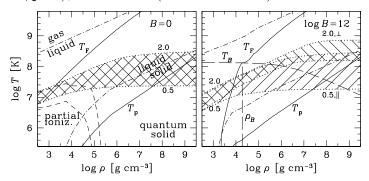


Fig. 1: Characteristic ρ –T domains for outer NS envelopes composed of iron. Left panel: non-magnetic plasma; right panel: $B=10^{12}$ G. Shown are ρ -dependences of $T_{\rm F}$, $T_{\rm p}$, $T_{\rm B}$, ρ_B (see text); lines where $\Gamma=1$ and $\Gamma=175$ (dot-dashed curves); lines where effective Z equals 15 or 20 (short-dashed lines on the left panel). Dotted lines and hatched regions show temperature profiles in NSs at different cooling stages and (on the right panel) at different inclinations of the magnetic field.

two dotted curves for each value of T_{s6} : the lower curve of each pair corresponds to the heat propagation along the field lines (\parallel , – i.e., near the magnetic poles) and the upper one to the transverse propagation (\perp , near the magnetic equator).

2 Equation of state

Thermodynamic functions of the electron gas at arbitrary degeneracy are expressed through the well known Fermi-Dirac integrals. For astrophysical use, it is convenient to employ analytic fitting formulae for these functions presented, e.g., in ref. [3].

Nonideal (exchange and correlation) corrections for nonrelativistic electrons at finite temperature have been calculated and parameterized in ref. [4]. For the relativistic electrons at low T, an analytic expansion of the exchange corrections is given, e.g., in ref. [5] (in this case, the correlation corrections are negligible). A smooth interpolation between these two cases has been constructed in ref. [6].

For the ionic component at $\Gamma \gg 1$, the main contribution to the thermodynamic functions comes from the ion correlations. Strongly coupled one-component Coulomb plasmas (OCP) of ions in the *uniform* electron background have been studied by many authors. The thermodynamic functions of the classical OCP liquid have been calculated [7, 8] at $\Gamma \geq 1$ and parameterized [3, 6] for $0 < \Gamma \lesssim 200$. The latter parameterization ensures accuracy $\sim 10^{-3}k_{\rm B}T$ (per particle).

For the classical Coulomb crystal, accurate numerical results and fitting formulae to the free energy F (with anharmonic corrections taken into account) have been presented in refs. [9, 10]. A comparison of the latter results with the fit [6] for the liquid yields the liquid–solid phase transition at $\Gamma_m = 175.0 \pm 0.4$ (curiously, this value

could be derived in ref. [7], but it was first noticed in ref. [6]).

In the solid phase, quantum effects may be important at the considered temperatures. These effects can be most easily taken into account in the approximation of a harmonic Coulomb crystal. A convenient analytic approximation is provided by a model [11] which treats two phonon modes as Debye modes and the third one as an Einstein mode. Numerical calculations [12] of the harmonic-lattice contributions to F, U, C_V , and the mean-square ion displacement are reproduced by this model at arbitrary T/T_p within several percent, which is sufficient for many applications.

Finally, there is a contribution from ion-electron (ie) correlations, which can be treated as polarization of the "jellium" of the degenerate electrons. In a Coulomb liquid, this contribution has been evaluated in refs. [13, 14] using a perturbation theory which involves the electron dielectric function and the static structure factor of ions. This approximation is justified at $k_{\rm TF} \ll k_{\rm F}$ (which is the case at $\rho_6 \gtrsim 10^{-2}$). At smaller densities the ie contribution in the Coulomb liquid has been calculated in ref. [3] using the HNC technique (heavy dots in Fig. 2).

In a Coulomb solid, the ie contribution has been evaluated in ref. [6] using the perturbation theory [13, 14] and a model lattice structure factor. These results, though approximate, indicate that the polarization corrections may be rather important. In particular, Γ_m may be shifted by $\sim 10\%$ when the ie

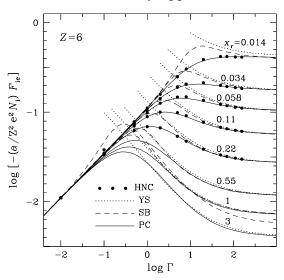


Fig. 2: Nonideal ie contribution to the free energy of carbon (normalized to $N_i(Ze)^2/a$, where N_i is the number of ions) at 8 values of x_r marked near the curves. HNC results [3] and relativistic perturbation theory [14] (YS) are compared with analytic fits [15] (SB) and [6] (PC).

corrections in the liquid and solid phases are taken into account.

The numerical results have been fitted [3, 6] by analytic functions of x_r and Γ . The approximation [6] for the OCP liquid is shown in Fig. 2 by solid lines. Since the *ie* correction is not dominant, the accuracy of the fitting formulae ($\lesssim 10\%$) is sufficient for most of astrophysical applications. An alternative Padé approximation, proposed in ref. [15] for the electron-ion fluid, is also accurate at $x_r \lesssim 1$ for small and large Γ , but it is less accurate at intermediate Γ and inapplicable at $x_r > 1$ (dashed lines).

As mentioned above, quantizing magnetic fields significantly affect the equation of state. In the fully ionized dense plasma, the main effects are described by the model of ideal electron gas, studied by many authors (e.g., [2, 16]).

3 Electron conductivities

Heat conduction in NS envelopes is provided mainly by the electrons. The thermal conductivity tensor κ is determined mainly by the electron-ion scattering. Calculation of κ should take into account specific features of the Coulomb plasmas in NS envelopes, quite different from the terrestrial liquid and solid metals: (i) in the liquid phase, an incipient long-range order emerges at $\Gamma \gtrsim 10^2$; (ii) in the solid phase, there are

usually many Brillouin zones within the Fermi surface; (iii) in the solid phase, the approximation of one-phonon scattering fails near the melting, which necessitates the use of a more general expression for the structure factor of ions. These features have been taken into account in ref. [17], where analytic approximations to the electron transport coefficients have also been derived.

Magnetic field hampers electron transport across the field lines: transverse thermal and electrical conductivities are reduced by orders of magnitude in typical NS envelopes. Strongly quantizing field significantly changes also longitudinal conductivities; weakly quantizing field causes de Haas-van Alphen oscillations. These effects have been outlined, e.g., in [2]. A unified treatment of the electron transport coefficients in the domains of classical, weakly quantizing, and strongly quantizing magnetic field has been developed in [18]. A Fortran code which implements this treatment is available at http://www.ioffe.rssi.ru/astro/conduct/. Using this code and solving the thermal diffusion equation, we have calculated the $T(\rho)$ profiles shown in Fig. 1.

Acknowledgements

AYP is grateful to the theoretical astrophysics group at Ecole Normale Supérieure de Lyon for generous hospitality and financial support. The work of AYP and DGY has been supported in part by INTAS (grant 96-542) and RFBR (grant 99-02-18099). AYP and DGY thank the Organizing Committee for support provided to attend PNP10.

References

- [1] YAKOVLEV, D.G., GNEDIN, O.Y., POTEKHIN, A.Y., this volume
- [2] Yakovlev, D.G., Kaminker, A.D., in The Equation of State in Astrophysics, ed. G. Chabrier, E. Schatzman, Cambridge Univ., Cambridge, UK (1994) 214
- [3] Chabrier, G., Potekhin, A.Y., Phys. Rev. E 58 (1998) 4941
- [4] ICHIMARU, S., IYETOMI, H., TANAKA, S., Phys. Rep. **149** (1987) 91
- [5] STOLZMANN, W., BLÖCKER, T., Astron. Astrophys., **314** (1996) 1024
- [6] POTEKHIN, A.Y., CHABRIER, G., Phys. Rev. E (2000) accepted
- [7] DEWITT, H., SLATTERY, W., CHABRIER, G., Physica B 228 (1996) 21
- [8] Caillol, J.M., J. Chem. Phys. 111 (1999) 6538
- [9] Dubin D.H.E., Phys. Rev. A **42** (1990) 4972
- [10] Farouki, R.T., Hamaguchi, S., Phys. Rev. E 47, 4330 (1993).
- [11] Chabrier, G., Astrophys. J. **414** (1993) 695
- [12] Baiko, D.A., Ph.D. thesis, Ioffe Phys.-Tech. Institute, St. Petersburg (2000)
- [13] GALAM, S., HANSEN, J.P., Phys. Rev. A 14 (1976) 816
- [14] Yakovlev, D.G., Shalybkov, D.A., Astrophys. Space Phys. Rev. 7 (1989) 311
- [15] STOLZMANN, W., BLÖCKER, T., Astron. Astrophys. (2000) accepted; astro-ph/0008399
- [16] Blandford, R.D., Hernquist, L., J. Phys. C 15 (1982) 6233
- [17] POTEKHIN, A.Y., BAIKO, D.A., HAENSEL, P., YAKOVLEV, D.G., Astron. Astrophys. **346** (1999) 345
- [18] POTEKHIN, A.Y., Astron. Astrophys. **351** (1999) 787